Обзор ArXiv/astro-ph, 15-27 апреля 2022

От Сильченко О.К.

ArXiv: 2204.12096

Galactic seismology: joint evolution of stellar and gaseous disc corrugations triggered by a crossing satellite

Thor Tepper-García,[1,2]★ Joss Bland-Hawthorn[1,2] and Ken Freeman[4]
[1]*Sydney Institute for Astronomy, School of Physics, University of Sydney, NSW 2006, Australia*
[2]*Centre of Excellence for All Sky Astrophysics in Three Dimensions (ASTRO-3D), Australia*
[4]*Mount Stromlo Observatory, Private Bag, Woden, ACT 2611, Australia*

Accepted —. Received —; in original form —

ABSTRACT

Evidence for wave-like corrugations are well established in the Milky Way and in nearby disc galaxies. These were originally detected as a displacement of the interstellar medium about the midplane, either in terms of vertical distance or vertical velocity. Over the past decade, similar patterns have emerged in the Milky Way's stellar disc. We investigate how these vertical waves are triggered by a passing satellite. For the first time, we use high-resolution N-body/hydrodynamical simulations to study how the corrugations set up and evolve jointly in the stellar and gaseous discs. We find that the gas corrugations follow the stellar corrugations, i.e. they are initially in phase although, after a few rotation periods (500-700 Myr), the distinct waves separate and thereafter evolve in different ways. The spatial and kinematic amplitudes (and thus the energy) of the corrugations dampen with time, with the gaseous corrugation settling at a faster rate (~ 800 Myr vs. ~ 1 Gyr). In contrast, the vertical energy of individual disc stars is fairly constant throughout the galaxy's evolution. This difference arises because corrugations are an emergent phenomenon supported by the collective, ordered motions of co-spatial ensembles of stars. We show that the damping of the stellar corrugations can be understood as a consequence of incomplete phase mixing, while the damping of the gaseous corrugations is a natural consequence of the dissipative nature of the gas. We suggest that the degree of correlation between the stellar and gaseous waves may help to age-date the phenomenon.

Key words: methods: analytic – Surveys – the Galaxy – stars: kinematics and dynamics – methods: N-body simulations –

Серия моделей MW AGAMA+RAMSES

Table 1. Galaxy model parameters. Columns 1 and 2 identify the galactic components and their associated functional forms; we note that these are approximations because they share the same gravitational potential. The total mass, scale length and cut-off radius are indicated in columns 3, 4, and 5 respectively. Column 6 is the number of collisionless particles used in the simulation (halo, bulge, disc) or to sample the gas disc distribution.

Component	Profile	Total mass $M_{\rm tot}$ (10^{10} $M_\odot$)	Radial scalelength r_s (kpc)	Cut-off radius r_c (kpc)	Particle count N (10^6)
DM halo	NFW	145	15	300	20
Stellar bulge	Hernquist	1.5	0.6	2.0	4.5
Stellar disc	Exp, sech^2	3.4	3.0	40	50
Gas disc	Exp, sech^2	0.4	7.0	–	2

Notes: The NFW and Hernquist functions are defined elsewhere (Navarro et al. 1997; Hernquist 1990). The scaleheight of the stellar disc is $z_d \approx 250$ pc; the Toomre local instability parameter of the stellar disc is everywhere $Q \gtrsim 1.3$. The gas disc is isothermal with $T = 10^3$ K, with a scaleheight that varies with radius from roughly 20 pc near the centre to 160 pc at $R = 20$ kpc (a 'flaring' disc). The gas disc is not truncated but merges smoothly with the background density (set at 10^{-20} cm^{-3} in our RAMSES setup).

Раскачка и звездного, и газового диска

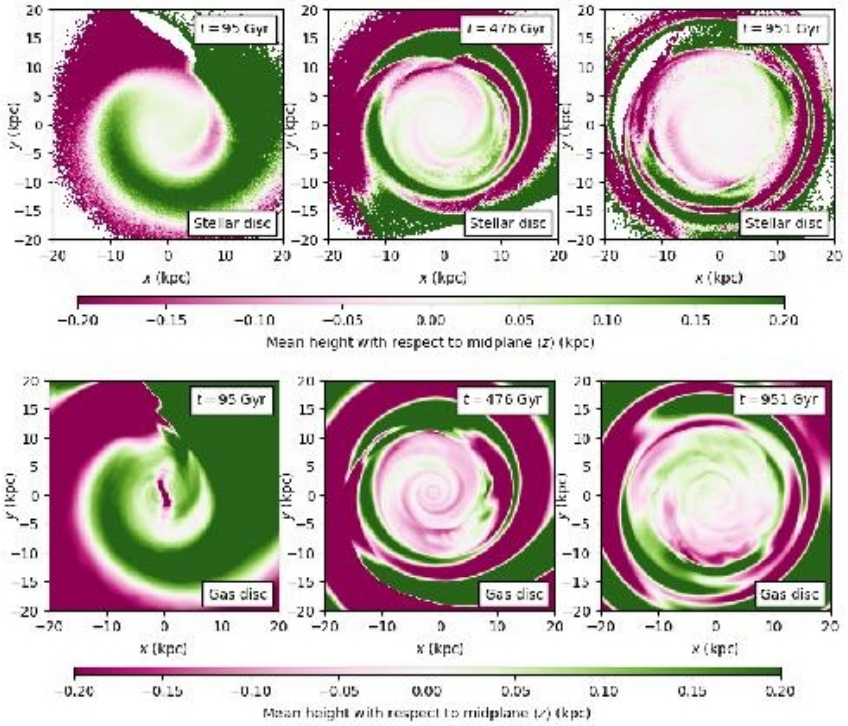

Figure 1. Mean height (in kpc) with respect to the galactic midplane of the stars in the disc (top) and gas (bottom) ~ 100 Myr after the impact (left), ~ 380 Myr after the impact (middle), and ~ 850 Myr after the impact (right) in the interaction hybrid simulation.

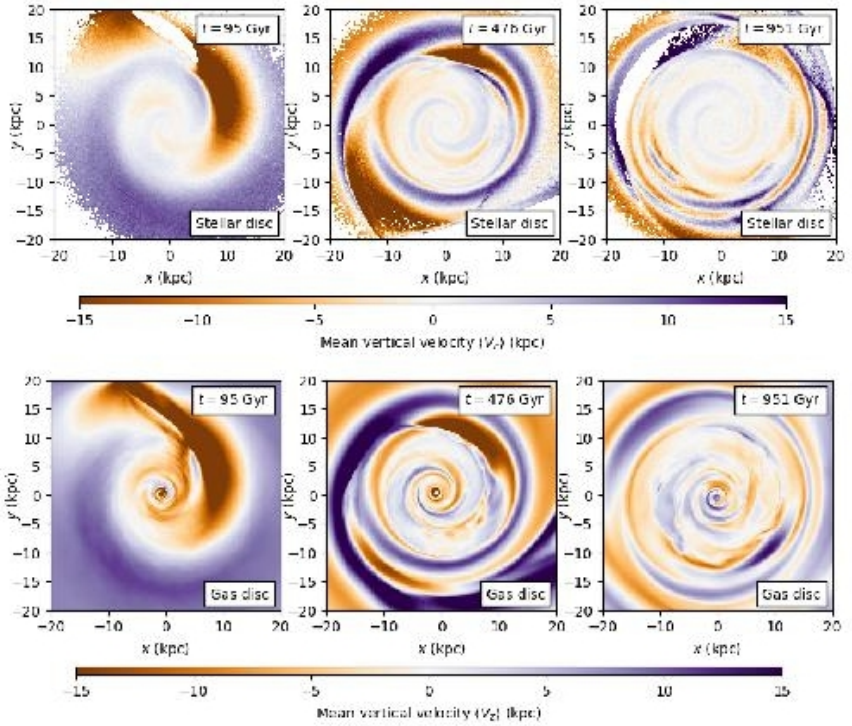

Figure 2. Mean vertical velocity of the stars in the disc (top) and gas (bottom) ~ 100 Myr after the impact (left), ~ 380 Myr after the impact (middle), and ~ 850 Myr after the impact (right) in the interaction hybrid simulation.

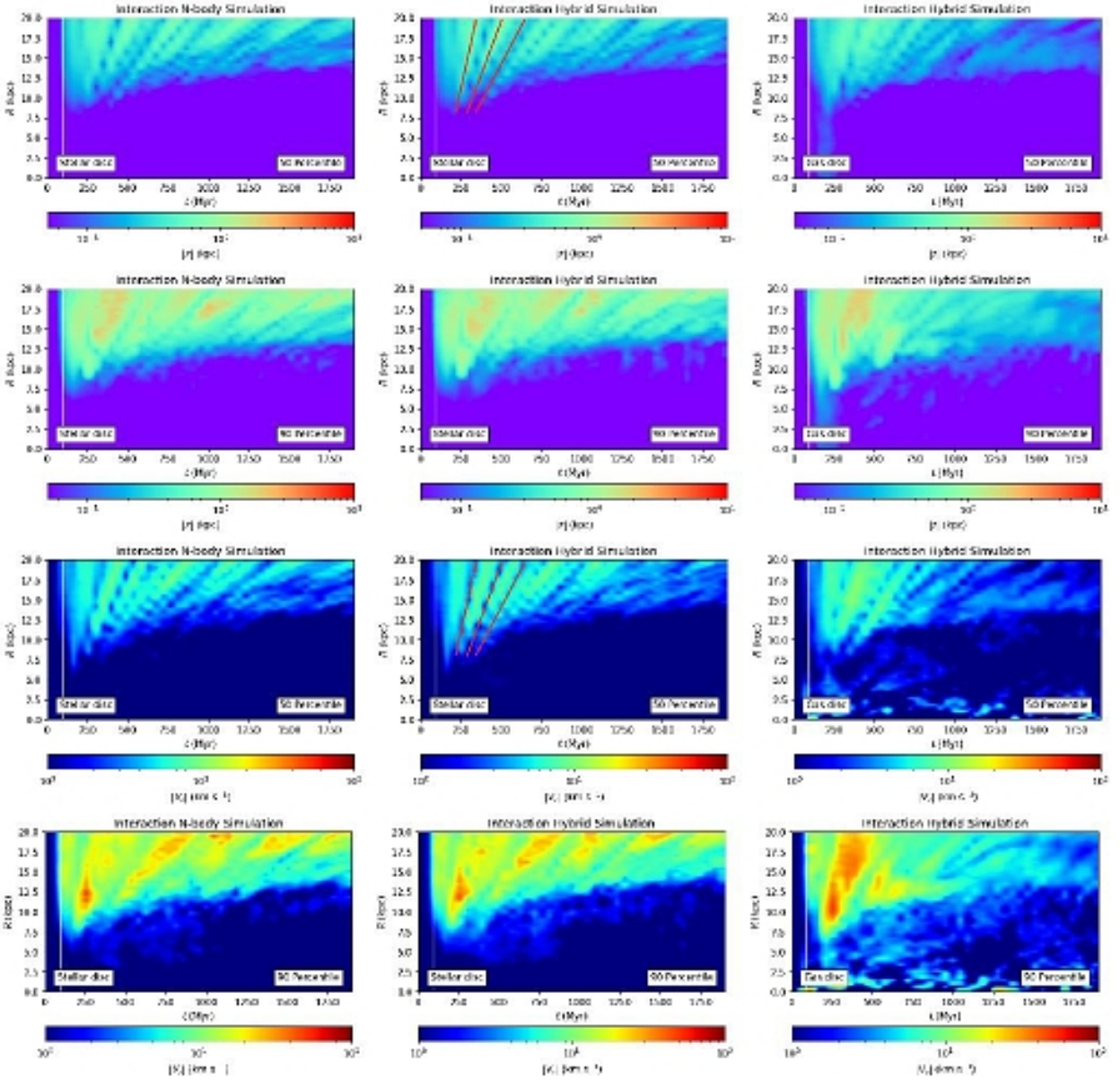

Figure 6. Spatial and kinematic amplitude of corrugations. Each panel displays the evolution in time of the absolute value of either the vertical displacement $|z|$ (in kpc; rows 1 and 2) or the vertical velocity $|V_z|$ (in km s^{-1}; rows 3 and 4) across the disc at each radius. The first and third rows display the amplitude in $|z|$ or $|V_z|$ at the 50 percentile level, respectively, while the second and fourth rows display these quantities at the 90 percentile level. The left column displays the results for the stellar disc in interaction N-body model, while the central column and right columns corresponds to the interaction hybrid model. The central column displays the result for the stellar disc, and the last column, the result for the gas disc. The white vertical line flags the epoch of the impact at $t \approx 100$ Myr and it is identical in all panels. The red lines in the rows 1 and 3 (central column) are identical and illustrate the fact that maxima in the vertical displacement are coincident with minima in the vertical velocity (and vice-versa). See text for further details.

Газовый и звездный диск качаются по-разному…

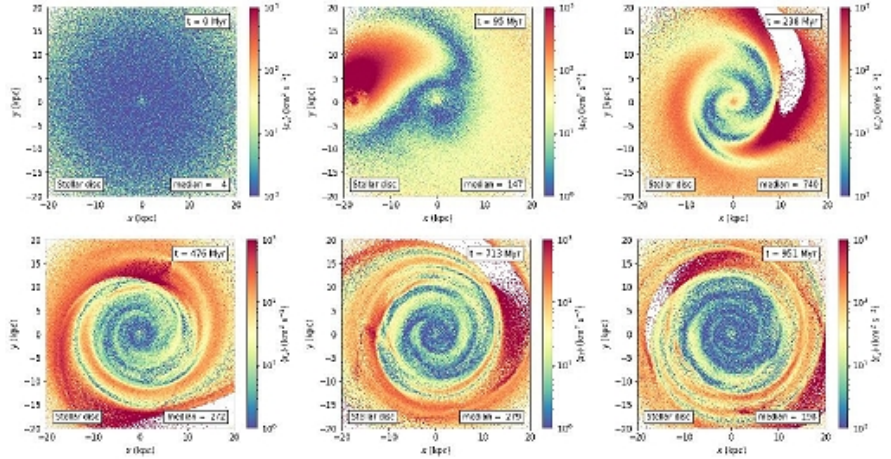

Figure 7. Vertical specific energy (Eq. 4) across the stellar disc in the interaction hybrid simulation from roughly 100 Myr prior to the impact to roughly 850 Myr after impact. Each panel corresponds to a selected time step, indicated on its top-right corner. The colour coding indicates the value of the mean vertical energy at each location across the disc. The median value of the energy (in $km^2\ s^{-2}$) across the entire disc in each snapshot is indicated on the bottom-right corner of each panel. Clearly, the vertical energy rises significantly around the impact epoch ($t \approx 100$ Myr), and it is generally higher at larger radii, regardless of the epoch. Note that the impact site is clearly visible at $x \approx -18$ kpc in the central panel, top row.

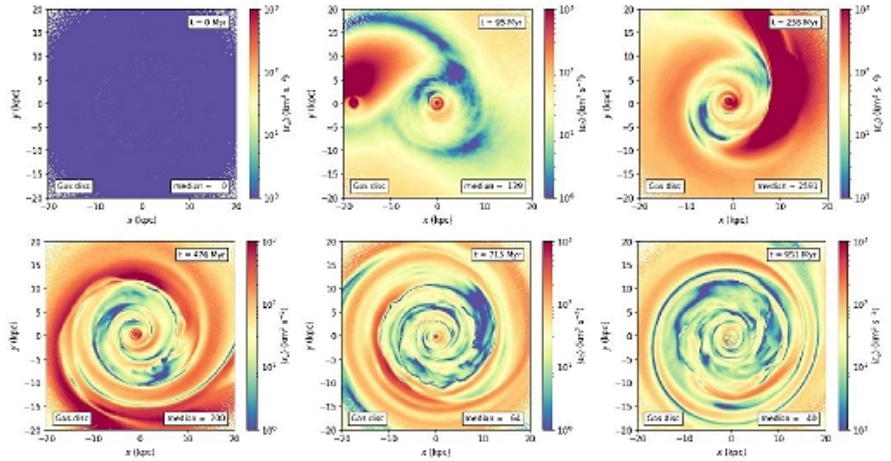

Figure 8. Same as Fig. 7, but for the gas disc. Note that the impact site is clearly visible at $x \approx -18$ kpc in the central panel, top row.

Но влияют друг на друга!

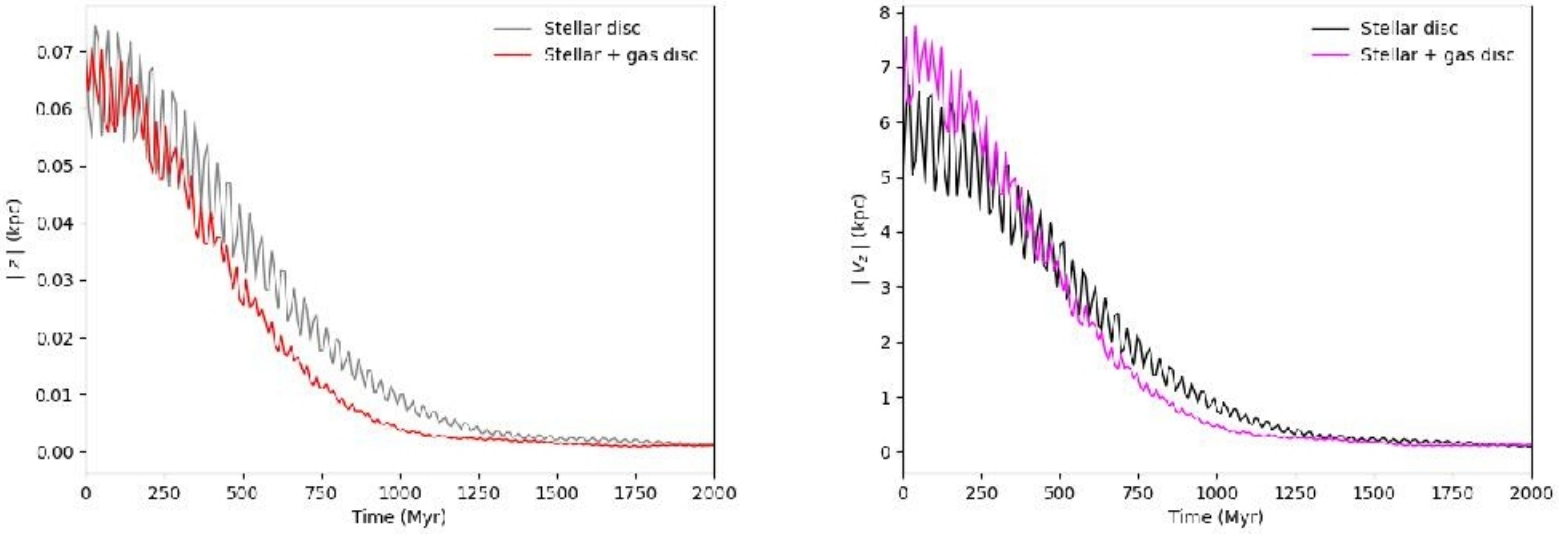

Figure 10. Evolution of the mean vertical amplitude (left) and mean vertical velocity (right) of an ensemble of stars undergoing phase mixing. Since the value of $|z|$ and $|V_z|$ oscillates with high frequency, we show instead the moving average of the actual signal calculated with a box-car window of width equivalent to 40 Myr. A stronger potential close to the midplane, originating from the combined effect of a stellar and a gaseous disc, results in a stronger damping of the spatial and kinematic amplitudes, compared to a stellar-only potential. See text for details.

Корреляция движений газа и звезд

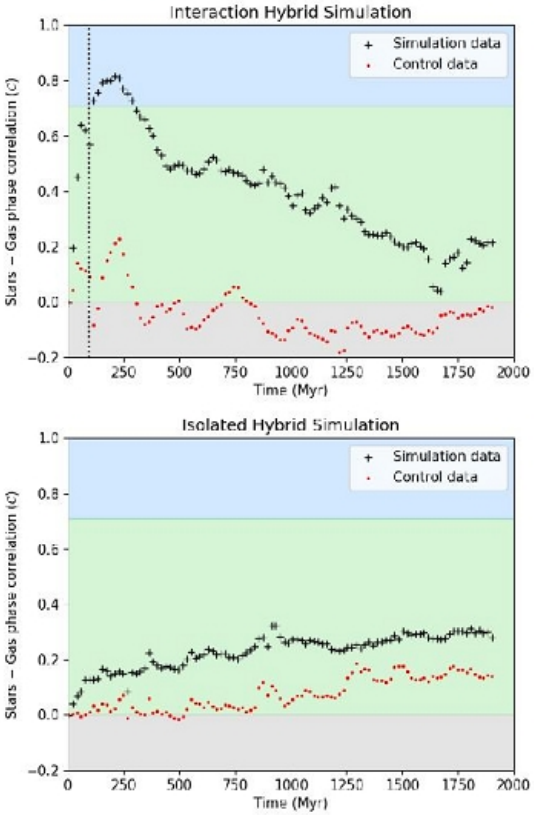

Figure 5. The evolution of the phase correlation C of the joint stellar and gas corrugations (Eq. 3) from roughly -100 Myr prior to the impact (tagged by the vertical dotted line) to roughly 1800 Myr after the impact is shown in the bottom-right panel (black '+' symbols). Top: Interaction hybrid simulation. Bottom: Isolated hybrid simulation. In both panels the red dots indicate the evolution of C for our control data. The blue / green / grey shaded areas follow the colour coding of Fig. 4 (see text for details).

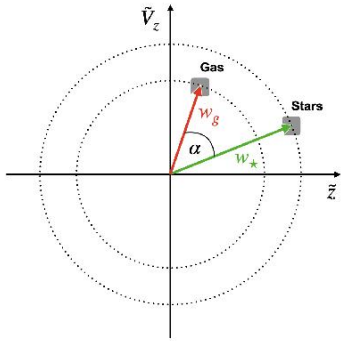

Figure 3. Schematic representation of the location in vertical phase-space of an ensemble of stars (pointed at by the green vector) and a patch of gas (pointed at by the red vector) found on a point (x, y) in the galaxy disc, and the angle (phase) difference, α, between these. Note that the phase space coordinates $(\tilde{z}, \tilde{V}_z)$ are rescaled versions of the counterparts (z, V_z) (Eq. 1).

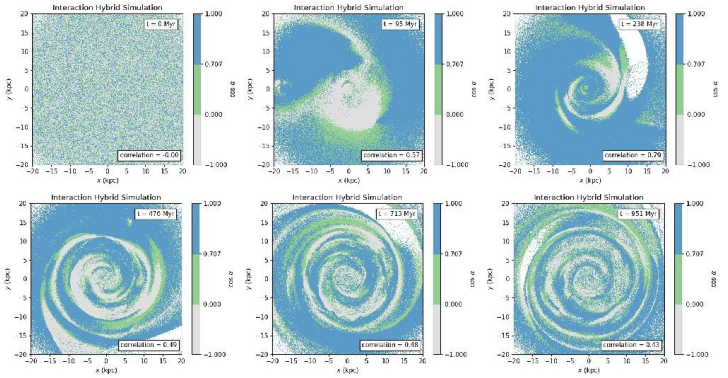

Figure 4. Evolution of the angle α between stars and gas (Eq. 2) at selected epochs from roughly -100 Myr prior to the impact to roughly 850 Myr after the impact in the interaction hybrid simulation. Each panel and each displays the cosine of α between the phase space vector of an ensemble of stars and a patch of gas around each location $p(x, y)$ (see Fig. 3). Highly correlated corrugations are identified by a uniform blue colour, while weakly correlated corrugations are identified by a uniform green colour. In contrast, a uniform grey colour, in contrast, indicates non-correlated or anti-correlated star-gas corrugations (see text for details). Each panel corresponds to a given epoch as indicated by the legend on the top-right corner. The total correlation C between the vertical oscillations of